Eulerian-Lagrangian Modeling of Forestry Residues Gasification in a Fluidized Bed

Jun Xie[1], Wenqi Zhong[1], Baosheng Jin[1], Ming Song[1], Yingjuan Shao[1,2] and Hao Liu[2]
[1]*Key Laboratory of Energy Thermal Conversion and Control of Ministry of Education, School of Energy and Environment, Southeast University, Nanjing 210096, China*
[2]*Institute of Sustainable Energy Technology, The University of Nottingham, Nottingham, U.K.*

Keywords: Forestry Residues, Fluidized Bed Gasifier, Numerical Simulation, Eulerian-Lagrangian Approach.

Abstract: A comprehensive three-dimensional model is developed to simulate forestry residues gasification in a fluidized bed gasifier using Eulerian-Lagrangian method. Both complex gas-solid flow and chemical reactions are considered. The model is based on the multiphase particle-in-cell (MP-PIC) method, which uses an Eulerian method for fluid phase and a discrete particle method for particle phase. Homogenous and heterogeneous chemistry are described by reduced-chemistry and the reaction rates are solved on the Eulerian grid. Simulations were carried out in a laboratory scale pine gasifier at different operating conditions. The predicted product gas contents and carbon conversion efficiency compare well with the experimental data. The formation of flow patterns, profiles of temperature and distributions of gas compositions were also obtained.

1 INTRODUCTION

within the fluid mixture were considered. Granular flow patterns, gas composition distributions and Biomass is important in energy conversion processes due to its favourable status with respect to greenhouse gas emissions (Nemtsov, 2008). Biomass materials known as potential sources of energy are agricultural residues such as straw, bagasse, and husk and residues from forest-related industries such as wood chips, sawdust, and bark (Nikoo, 2008).

Fluidized bed gasifiers are advantageous for transforming biomass, particularly agricultural and forestry residues, into energy. Advantages of fluidization include high heat transfer, uniform and controllable temperatures, perfect gas–solid contacting and the ability to handle a wide variation in particulate properties (Nemtsov, 2008; Nikoo, 2008).

Over the last decade computational fluid dynamic (CFD) models have been applied to biomass gasifier. There are two approaches: Eulerian-Eulerian models (EEM) and Eulerian-Lagrangian models (ELM). The ELM tracks each individual fuel particle, making it possible to include the changes in physico-chemical characteristics of the fuel particle during devolatilization and subsequent char conversion. There are some models for biomass conversion employing ELM in entrained-flow gasifiers. Little work has been found using ELM to simulate biomass gasification in a fluidized bed because of the computational complexity of calculating dense particle-particle interactions. If coupled with chemical reactions, this application is computationally more expensive (Barea, 2010).

The objective of this study is to develop a comprehensive three-dimensional numerical model for fluidized bed coal gasification. The methodology describes the dense gas-solid flow on a basis of multiphase particle-in-cell (MP-PIC). The method is a form of Eulerian-Lagrangian approach, where each particle has three-dimensional forces from fluid drag, gravity, static-dynamic friction, particle collision and possibly other forces (Snider, 2007). Homogenous and heterogeneous chemistry are described by reduced-chemistry and the reaction rates are solved numerically on the Eulerian grid. Complex particle and gas flow, mass and heat transfer, chemical reactions between phases and other important characteristics were obtained at different operating conditions. The calculated product gas compositions and carbon conversion efficiency compare with the experimental data to confirm the validity of the

Xie J., Zhong W., Jin B., Song M., Shao Y. and Liu H..
Eulerian-Lagrangian Modeling of Forestry Residues Gasification in a Fluidized Bed.
DOI: 10.5220/0004013802970302
In *Proceedings of the 2nd International Conference on Simulation and Modeling Methodologies, Technologies and Applications* (SIMULTECH-2012), pages 297-302
ISBN: 978-989-8565-20-4

model.

2 NUMERICAL MODELS

2.1 Governing Equations for Gas Phase

The gas dynamics is described by averaged Navier-Stokes equations with strong coupling with the particle phase. The large eddy simulation (LES) turbulence model is adopted. Mass, momentum and energy of the two-phase mixture are conserved by exchange terms which can be included in the mass, momentum and energy conservation equations, respectively (Snider, 2011&2001).

$$\frac{\partial(\theta_g \rho_g)}{\partial t} + \nabla \cdot (\theta_g \rho_g u_g) = \delta \dot{m}_p \quad (1)$$

$$\frac{\partial(\theta_g \rho_g u_g)}{\partial t} + \nabla \cdot (\theta_g \rho_g u_g u_g) = -\theta_g \nabla p + F + \theta_g \rho_g g + \nabla \cdot (\theta_g \tau_g) \quad (2)$$

where u_g, θ_g and ρ_g represent the gas velocity vector, volume fraction and density, respectively. $\delta \dot{m}_p$ is the gas mass production rate per volume from particle-gas chemistry. The terms p, τ_g and g are the mean flow gas thermodynamic pressure, stress tensor and gravitational acceleration. F is the rate of momentum exchange per volume between the gas and particle phases.

As a form of energy equation, the enthalpy equation is

$$\frac{\partial}{\partial t}(\theta_g \rho_g h_g) + \nabla \cdot (\theta_g \rho_g h_g u_g) = \theta_g \left(\frac{\partial p}{\partial t} + u_g \cdot \nabla p \right) + \phi - \nabla \cdot (\theta_g q) + \dot{Q} + S_h + \dot{q}_D \quad (3)$$

Where h_g is the gas enthalpy; ϕ is the viscous dissipation; and $\dot{Q}$ is an energy source per volume. In this work, the viscous dissipation is ignored, and there is no energy source. q is the fluid heat flux and $\dot{q}_D$ is the enthalpy diffusion term. The term S_h represents the conservative energy exchange from the particle phase to the gas phase.

The gas phase is a multicomponent mixture. Through recombining chemical bonds of molecules and atoms, mass is transferred between gas species, which is represented as chemical source term $\delta \dot{m}_{i,chem}$. The transport equation for individual gas species is

$$\frac{\partial(\theta_g \rho_g Y_{g,i})}{\partial t} + \nabla \cdot (\theta_g \rho_g Y_{g,i} u_g) = \nabla \cdot (\rho_g D \theta_g \nabla Y_{g,i}) + \delta \dot{m}_{i,chem} \quad (4)$$

where D is the turbulent mass diffusivity which is related to the viscosity by the Schmidt number correlation $\mu/\rho_g D = Sc$. Sc is set as 0.9.

2.2 Governing Equations for Solid Phase

The methodology is a form of Eulerian-Lagrangian method, in which the dynamics of the particle phase is calculated by solving a transport equation for the particle distribution function (PDF) f. The transport equation for the PDF is derived from Boltzmann-BGK model of gas dynamics. And some improvements were made for collision damping time which includes the effects of the particle material coefficient of restitution and non-equilibrium particle velocity distributions. For simplicity, it is assumed that f is a function of particle spatial location x_s, particle velocity u_s, particle mass m_s, particle temperature T_s and time t. Thus $f(x_s, u_s, m_s, T_s, t)$ $du_s dm_s dT_s$ is the average number of particles per unit volume with velocities in the interval (u_s, u_s+du_s), mass in the in the interval (m_s, m_s+dm_s), and temperature in the interval (T_s, T_s+dT_s) (Snider, 2011).

The transport equation for f is

$$\frac{\partial f}{\partial t} + \frac{\partial (fv)}{\partial x} + \frac{\partial (fA)}{\partial v} = \frac{f_D - f}{\tau_D} \quad (5)$$

where A is the particle acceleration; f_D is the PDF for the local mass-averaged particle velocity; and τ_D is the collision damping time.

$$A = D_s(u_g - u_s) - \frac{1}{\rho_s}\nabla p - \frac{1}{\theta_s \rho_s}\nabla \tau_s + g + Fs \quad (6)$$

where D_s is the drag function which depends on the particle size, velocity, position and time. θ_s, ρ_s and τ_s are the solids volume fraction, mass density and contact normal stress, respectively. The particle friction per mass, Fs is opposite and limited to the relative particle motion.

Particle-to-Particle collisions are modeled by the particle normal stress which is an approximation of collective effects of neighbor particles on a particle. The MP-PIC method makes use of spatial gradients because they are readily calculated on the Eulerian grid and then apply the gradient to discrete particles. The particle stress is derived from the particle volume fraction which is in turn calculated from particle volume mapped to the grid. The particle

normal stress model used here is

$$\tau = \frac{P_s \theta_s^{\beta}}{\max\left[(\theta_{cs} - \theta_s), \varepsilon(1-\theta_s)\right]} \tag{7}$$

where the constant P_s has units of pressure, and θ_{cs} is the particle volume fraction at close packing. β is the constant, $2 \leq \beta \leq 5$. The ε is a small number on the order of 10^{-7} to remove the singularity.

The particles volume fraction is defined by f

$$\theta_s = \iiint f \frac{m_s}{\rho_s} dm_s du_s dT_s \tag{8}$$

and the gas volume fraction is $\theta_g = 1 - \theta_s$.

The conservative mass, momentum and energy exchange between gas and solid phases are presented as follows

$$\delta \dot{m}_s = -\iiint f \frac{dm_s}{dt} dm_s du_s dT_s \tag{9}$$

$$F = -\iiint f \left\{ m_s \left[D_s (u_g - u_s) - \frac{\nabla p}{\rho_s} \right] + u_s \frac{dm_s}{dt} \right\} dm_s du_s dT_s \tag{10}$$

$$S_h = \iiint f \left\{ m_s \left[D_s (u_s - u_g)^2 - C_V \frac{dT_s}{dt} \right] - \frac{dm_s}{dt} \left[h_s + \frac{1}{2}(u_s - u_g)^2 \right] \right\} dm_s du_s dT_s \tag{11}$$

In which, h_s is the particle enthalpy. The energy from the solid is the sensible heat and the heat of formation.

2.3 Chemical Reaction Models

In the MP-PIC method, we use a cell-average chemistry calculation. By interpolating discrete computational particle properties to the grid, average properties of the particle phase are got for the chemical rate equations. The reaction rates are calculated in each grid cell. The total consumption rate of solids is defined by the reaction rates. The time rate of change of mass of individual particles dm_s/dt is related to the total rate of change of molar concentration of solid carbon $d[C(s)]/dt$ by the volume of the particles (Snider, 2011).

$$\frac{dm_s}{dt} = \frac{\theta_g M w_c}{\rho_s \theta_s} m_s \frac{d\left[C(s)\right]}{dt} \tag{12}$$

where Mw_c is the molecular weight of carbon.

In our present work, we assumed that forestry residues devolatilization takes place instantaneously and volatile products consist of CO, CO_2, H_2O, H_2, CH_4, and C_2H_4. The quantities of these compositions are determined based on some experimental support, as well as the proximate and elemental analysis (Thunman, 2001). For the sake of simplification, reactions with sulfur are ignored for their little amount. Char only contains carbon.

Table 1: Chemical equations and reaction rates (Snider, 2011; de Souza-Santos, 2004).

Stoichiometric equation	Reaction rate expression / mol m^{-3} s^{-1}
$C+H_2O \rightarrow CO+H_2$	$r_1=1.272 m_s T \exp(-22645/T)\ [H_2O]$
$CO+H_2 \rightarrow C+H_2O$	$r_2=1.044\times10^{-4} m_s T^2 \exp(-6319/T-17.29)[CO]\ [H_2]$
$C+CO_2 \rightarrow 2CO$	$r_3=1.272 m_s T \exp(-22645/T)\ [CO_2]$
$2CO \rightarrow C+CO_2$	$r_3=1.044\times10^{-4} m_s T^2 \exp(-2363/T-20.92)[CO]_2$
$0.5C+H_2 \rightarrow 0.5CH_4$	$r_4=1.368\times10^{-3} m_s T \exp(-8078/T-7.087)[H_2]$
$0.5CH_4 \rightarrow 0.5C+H_2$	$r_5=0.151 m_s T^{0.5} \exp(-13578/T-0.372)[CH_4]^{0.5}$
$C+O_2 \rightarrow 2CO$	$r_6=4.34\times10^{7} \theta_p T \exp(-13590/T)[O_2]$
$CO+H_2O \rightarrow CO_2+H_2$	$r_7=7.68\times10^{10} T \exp(-36640/T)\ [CO]^{0.5}[H_2O]$
$CO_2+H_2 \rightarrow CO+H_2O$	$r_8=6.4\times10^{9} T \exp(-39260/T)\ [H_2]^{0.5}[CO_2]$
$CO+0.5O_2 \rightarrow CO_2$	$r_9=5.62\times10^{12} \exp(-16000/T)\ [CO][O_2]^{0.5}$
$CH_4+2O_2 \rightarrow CO_2+2H_2$	$r_{10}=3.552\times10^{11} \exp/T(-15700/T)[CH_4][O_2]$
$C_2H_4+3O_2 \rightarrow 2CO_2+2H_2$	$r_{11}=3.552\times10^{11} \exp/T(-15700/T)[C_2H_4][O_2]$
$H_2+0.5O_2 \rightarrow H_2O$	$r_{12}=1.63\times10^{11} \exp T^{-1.5}(-3430/T)[H_2]^{1.5}[O_2]$
$CH_4+H_2O \rightarrow CO+3H_2$	$r_{13}=3\times10^{5} \exp(-12500/T)[CH_4][H_2O]$

There are thousands of chemical reactions in a gasifier. A set of fourteen reactions describe the major conversion rates in the reactor. The solids are consumed and the particles shrink by heterogeneous chemistry reactions of combustion, gasification and methanation. The homogeneous reactions include carbon monoxide, hydrogen and methane combustion, water-gas shift and methane steam reforming reactions. The fourteen chemical reactions, together with the reaction rate expressions, are listed in Table 1.

2.4 Computational Setup

This simulated object is a lab-scale fluidized bed gasifier whose details can be found elsewhere (Lv, 2004). A schematic diagram of the reactor and the simulation grid are shown in Fig. 1. The experimental setup parameters and the operating conditions appear in Table 2. At the outlet, gas phase adopts out-flow boundary condition and no particle exit. The reactor is initially filled with N_2 and the silica sand is in the vessel with the volume fraction grids of 0.48 (Wang, 2009). To prevent excessive compression of particles, we set the solid close pack volume fraction as 0.5. The particle normal-to-wall momentum retention coefficient is 0.2 and the tangent–to-wall retention coefficient is 0.99. The time step of 2.0×10^{-4}s is used.

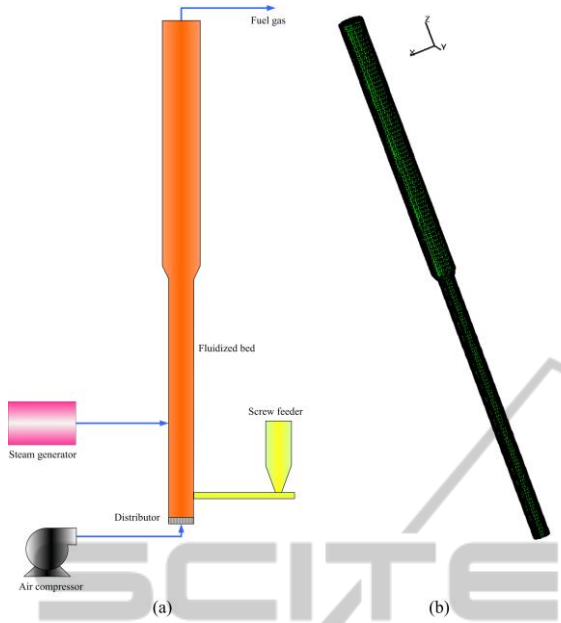

Figure 1: Schematic of the gasifier and simulation grid.

Table 2: Experimental setup parameters and operating conditions.

Fluidized bed reactor	
Temperature (℃)	750,800,850
Pressure (Pa)	101325
Bed diameter (mm)	40
Freeboard diameter (mm)	60
Height (mm)	1400
Air	
Temperature (℃)	65
Flow rate (Nm^3/h)	0.5
Steam	
Temperature (℃)	154
Flow rate (kg/h)	1.2
Feed material: Pine sawdust	
Particle diameter (mm)	0.3-0.45
Absolute density (kg/m3)	556
Char density (kg/m3)	1300
Flow rate (kg/h)	0.445
Bed material : Silica sand	
Particle diameter (mm)	0.2-0.3
Weight (g)	30g

3 RESULTS AND DISCUSSION

3.1 Flow Patterns

In the fluidized bed, air was used as the fluidizing agent and introduced into the reactor below the distributor. The particles include three species: silica sand, carbon and ash. The formation and development of granular flow regimes are illustrated with particle volume fraction in Fig. 2. As shown in Fig. 2(a)-(f), the particles tend to rise with time driven by gas-particle interactions. The particle concentration decreases along the reactor height.

3.2 Comparisons with Experiments

The present developed model was applied to three cases with different operating temperatures. Fig. 3 portrays the product gas composition of calculations and experiment data. All species are dry-gas molar contents.

Fig. 3(a)-(c) shows the predicted results compare well with the experimental data. The minimum relative error is less than 1%, and the maximum relative error is about 20%. The average relative error is less than 12%.Very little difference is found between predicted and measured H_2, CH_4 and C_2H_4 contents. The H_2 concentrations increase with increasing temperature and the contents of CH_4 show an opposite trend. Higher temperature favors the endothermic reaction of methane steam reforming.

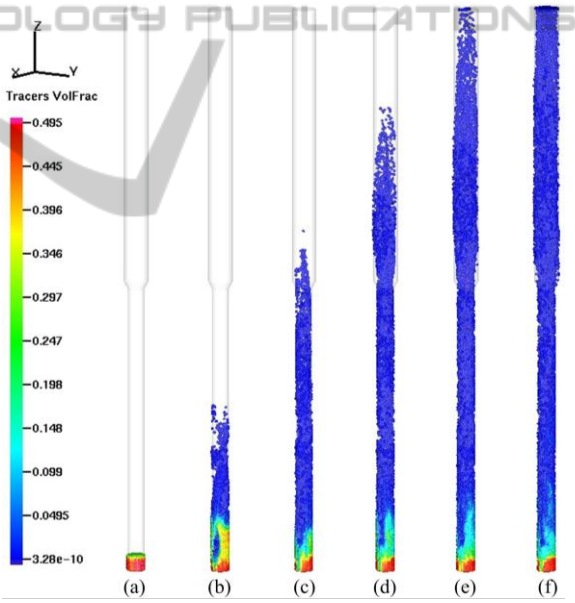

Figure 2: Flow patterns transition with time: (a) t=0s, (b) t=0.25s, (c) t=0.5s, (d) t=0.75s, (e) t=1.0s, (f) t =1.25s.

One or two calculation error of CO and CO_2 molar contents are more than 15%. The reason for these deviations is likely to be the simplified distribution coefficient of reactions: $C + \beta O_2 \rightarrow (2-\beta)\ CO_2 + (2-2\beta)\ CO$ and $C + \alpha H_2O \rightarrow (2-\alpha)\ CO + (\alpha-1)\ CO_2 + \alpha H_2$, the coefficients, α and β, change with temperature which are set as constants in our model. Part of the deviation comes from the neglect of tar production.

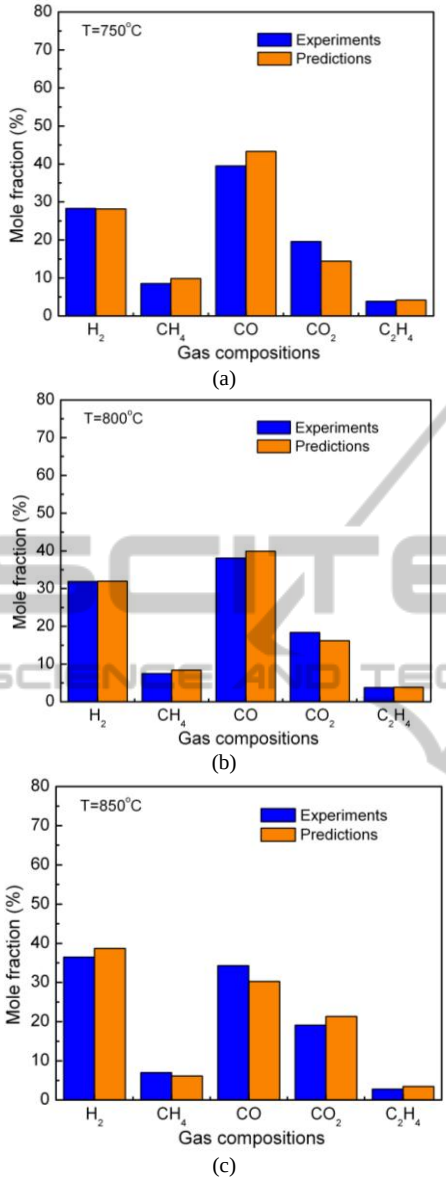

Figure 3: Comparisons between species mole contents predicted by model and experimental data.

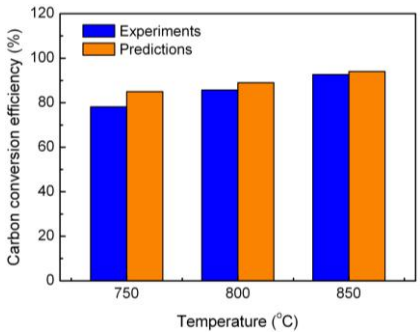

Figure 4: Comparisons between carbon conversion efficiency predicted by model and experimental data.

Fig. 4 compares the predicted carbon conversion efficiency with the measured data. Higher temperature improves the gasification process and increases the carbon conversion. There is good agreement between the simulation and experimental results. The average relative difference is only about 5%. Biomass produces tar and other light hydrocarbon (C_xH_y) in pyrolysis and gasification process. The present model did not consider the tar and light hydrocarbon, which is the main reason for over-estimation of carbon conversion efficiency.

3.3 Distributions of Gas Compositions

Fig. 5 displays the distributions of particle and gas temperatures in the reactor (a half slice at y=0). In general, the temperature in the bed region is higher than in the freeboard for the more contact of gasifying agent and fuel. The steam injection affects the temperature profile and lowers the temperature above the injection level. The peak temperatures are observed in the lower part of the bed, where the highest intensities of combustion and gasification reactions are located.

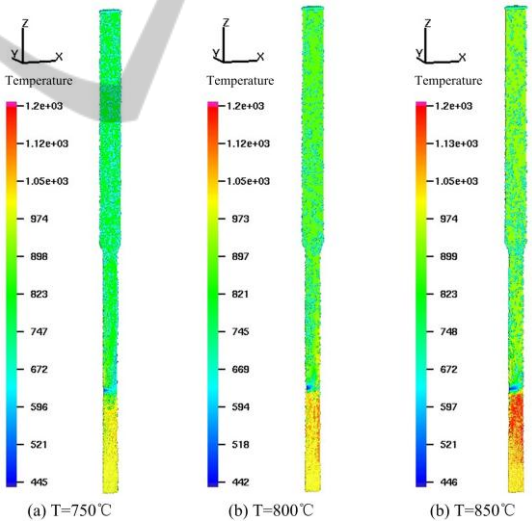

Figure 5: Distributions of particle and gas temperatures.

Fig. 6 illustrates the molar fraction distribution of the five most important gas species in the reactor (a half slice at y=0). It can be seen from the figure: the positions of the sawdust feeder and steam injector influence the gas profile. Near the particle inlet level, the molar concentrations of CO are highest due to the existence of a large number of carbon particle and devolatilization. The CO_2 concentrations remain almost constant along the whole height of the reactor for the homogeneous combustion reaction and

water-gas shift reaction. The overall trend of H_2, CH_4 and C_2H_4 contents is consistent. As a result of devolatilization, the peak concentrations of them are presented close to the feeder. Nevertheless, H_2 molar contents are higher than those of CH_4 and C_2H_4 in the freeboard region due to water-gas shift reaction and methane steam reforming reaction.

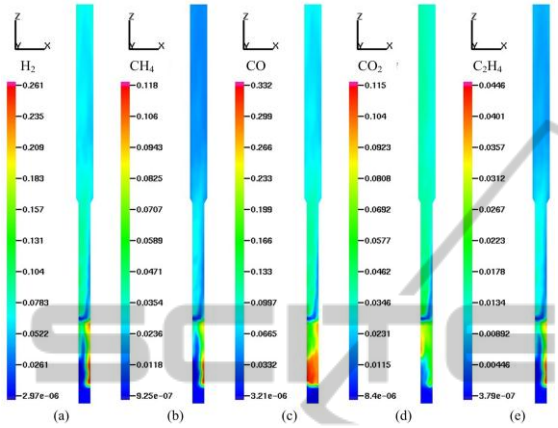

Figure 6: Molar fraction distributions of gas compositions (T=800℃).

4 CONCLUSIONS

A three-dimensional Eulerian-Lagrangian numerical model was developed to study the forestry residues gasification in a laboratory scale fluidized bed gasifier. By the simulations at different operating temperaures, gasifier's behavior was effectively predicted, including the complex particle flow patterns, profile of temperature and distributions of gas composition. The predicted product gas contents and carbon conversion efficiency compared well with experimental data. The present mathematical model can be a tool to explore the complex gas-solid flow and chemical reaction characteristics of fluidized bed gasification.

ACKNOWLEDGEMENTS

Financial supports from the Major State Basic Research Development Program of China (NO. 2011CB201505), China MOST for Inter-government S&T Optional Cooperation between China and Europe (2010DFA61960), NSFC (No. 51076029), and UK EPSRC for Collaboration Project of China and British (EP/G063176/1) were sincerely acknowledged.

REFERENCES

Nemtsov, D. A., Zabaniotou, A., 2008. Mathematical modelling and simulation approaches of agricultural residues air gasification in a bubbling fluidized bed reactor. *Chemical Engineering Journal* 143, 10–31.

Nikoo, M. B., Mahinpey, N., 2008. Simulation of biomass gasification in fluidized bed reactor using ASPEN PLUS. *Biomass and Bioenergy* 32, 1245–1254.

Gómez-Barea, A., Leckner, B., 2010. Modeling of biomass gasification in fluidized bed. *Progress in Energy and Combustion Science* 36, 444-509.

Snider, D. M., 2001. An incompressible three dimensional multiphase particle-in-cell model for dense particle flows. *Journal of Computational Physics* 170, 523-549.

Snider, D. M., 2007. Three fundamental granular flow experiments and CPFD predictions. *Powder Technology* 176, 36-46.

Snider, D. M., Clark, S. M., O'Rourke, P. J., 2011. Eulerian-Lagrangian method for three-dimensional thermal reacting flow with application to coal gasifiers. *Chemical Engineering Science* 66, 1285-1295.

Thunman, H., Thunman, H., Niklasson, F., Johnsson, F., Leckner, B., 2001. *Composition of Volatile Gases and Thermochemical Properties of Wood for Modeling of Fixed or Fluidized Beds*. Energy Fuels 15, 1488-1497

de Souza-Santos, M. L.,. Modeling, Simulation, and Equipment Operations. 2004. Marcel Dekker, Inc.

Lv, P. M., Xiong, Z. H., Chan, g J., Wu, C. Z., Chen, Y., Zhu, J. X., 2004. An experimental study on biomass air–steam gasification in a fluidized bed. *Bioresource Technology* 95, 95-101.

Wang, X. F., Jin, B. S., Zhong, W. Q., 2009. Three-dimensional simulation of fluidized bed coal gasification. *Chemical Engineering and Processing* 48, 695-705.